ELSEVIER

Applied Surface Science 161 (2000) 178–186

applied surface science

www.elsevier.nl/locate/apsusc

Multifunctional molecular materials combining photoelectric conversion and second-order optical nonlinearities in LB monolayer films

Fuyou Li [a], Jie Zheng [b], Chunhui Huang [b,1], Linpei Jin [a,*], Yanyi Huang [b],
Jianquan Guo [a], Tingting Liu [c], Xinsheng Zhao [c]

[a] *Department of Chemistry, Beijing Normal University, Beijing 100875, People's Republic of China*
[b] *State Key Laboratory of Rare Earth Materials Chemistry and Applications, Peking University, Beijing 100871, People's Republic of China*
[c] *Department of Chemistry, Peking University, Beijing 100871, People's Republic of China*

Received 21 December 1999; accepted 5 March 2000

Abstract

A series of multifunctional dye molecules with different relative positions of electron-accepting group, (*E*)-*N*-methyl-4-[2-(4-*N*-methyl-*N*-hexadecylaminophenyl) ethenyl]-2-quinolinium iodide (MHQ-2), (*E*)-*N*-methyl-4-[2-(4-*N*-methyl-*N*-hexadecylaminophenyl)ethenyl]-4-quinolinium iodide (MHQ-4) and (*E*)-*N*-methyl-4-[2-(4-*N*-methyl-*N*-hexadecylaminophenyl)ethenyl]-6-quinolinium iodide (MHQ-6) were synthesized. These amphiphilic dye molecules were successfully transferred onto ITO electrode or quartz by Langmuir–Blodgett (LB) technique. The second-harmonic generation (SHG) and photoelectric conversion (PEC) properties of their monolayers were studied under identical conditions. The sequence of $\chi^{(2)}$ and the photocurrent external quantum yield under the same conditions is MHQ-4 > MHQ-2 > MHQ-6, implying that the relative position of acceptor plays an important role in SHG and PEC properties. © 2000 Elsevier Science B.V. All rights reserved.

Keywords: Multifunctional materials; LB monolayers; SHG; PEC

1. Introduction

In the last decade, many researches focused on organic materials containing donor–π-acceptor conjugation systems, because they have high nonlinear polarizability. This kind of molecular structure facilitates an intramolecular photoinduced electron-transfer reaction between donor and acceptor through π-electron bridge with strong polarity effect and may produce considerable photoelectric conversion (PEC), photorefractive effect, nonlinear optical (NLO) effect [1,2]. Some organic materials combining magnetism [3–5] or conductivity [6,7] with NLO properties have already been reported. We have systematically studied the PEC properties of some organic material molecules with second-order NLO properties [8–12]

---

[*] Corresponding author.
[1] Also a corresponding author.

PII: S0169-4332(00)00296-8

and have found that there is a correlation between PEC and second-harmonic generation (SHG) properties, and now we focus on the relationship of the chemical structure and PEC property. The relationship between the SHG property and structure of organic molecules has been studied by experiments [13,14] and model calculations [15,16], and the effect of *o*-, *m*- and *p*-substitution of various nitroaniline on the SHG property was investigated [17]. However, to our knowledge, there is no report on the effect of different substituted positions of the same acceptor group on the PEC property. In fact, the effect of relative position of the acceptor substituents cannot be negligible. As part of our systematic studies, in this paper, three hemicyanine congeners with different relative positions of the acceptor group, (*E*)-*N*-methyl-4-[2-(4-*N*-methyl-*N*-hexadecylamino phenyl)ethenyl]-2-quinolinium iodide (MHQ-2), (*E*)-*N*-methyl-4-[2-(4-*N*-methyl-*N*-hexadecylaminophenyl)ethenyl]-4-quinolinium iodide (MHQ-4) and (*E*)-*N*-methyl-4-[2-(4-*N*-methyl-*N*-hexadecylaminophenyl)ethenyl]-6-quinolinium iodide (MHQ-6) were designed and synthesized (see Scheme 1). These dye molecules were successfully transferred onto ITO electrode or quartz by Langmuir–Blodgett (LB) technique. Their PEC and SHG properties were studied under identical conditions in order to investigate the effect of the electron acceptor with different relative positiona of quinolinium on the SHG and PEC properties. Mechanistic models for PEC under different conditions are proposed.

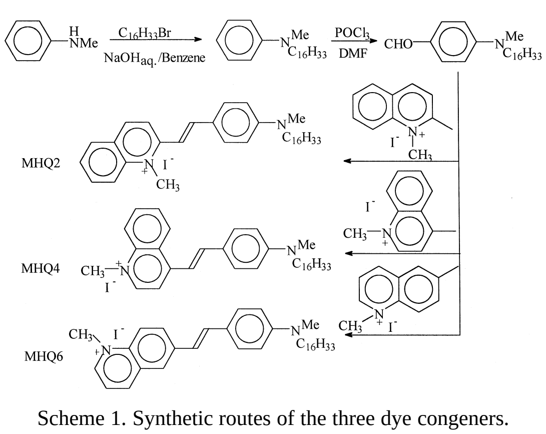

Scheme 1. Synthetic routes of the three dye congeners.

2. Experimental section

The synthesis of these dyes has closely followed the aldol condensation strategy [18]. MHQ-2 was synthesized by condensing 1,2-dimethyl quinolinium iodide with an equivalent mole of *N*-methyl-*N*-hexadecylaminobenzaldehyde [19] in absolute ethanol using piperidine as the catalyst. The product was purified by column chromatography on silica gel with a chloroform–methanol mixture (12:1) as eluent. MHQ-4 and MHQ-6 were synthesized following the same procedure as MHQ-2.

MHQ-2: Yield: 48%. M.p.: 182°C. Anal. Calc. for $C_{35}H_{51}N_2I$: C, 67.08; H, 8.20; N, 4.48. Found: C, 66.96; H, 8.25; N, 4.07. δ H (300 MHz, $CDCl_3$): 0.86 (t, 3 H, $1CH_3$), 1.24 (m, 26H, $13CH_2$), 1.53 (m, 2H, $1CH_2$), 2.93 (s, 3H, $1N{-}CH_3$), 3.25 (t, 2H, $1N{-}CH_2$), 4.57 (s, 3H, $1N^+{-}CH_3$), 6.68 (d, 2H, phenyl), 7.56 (d, 1H, CH=), 7.65 (d, 1H, phenyl), 7.87 (d, 1H, 1CH=), 7.93 (m, 2H, quinolyl), 8.08 (m, 2H, quinolyl), 8.56 (m, 2H, quinolyl).

MHQ-4: Yield: 76%. M.p.: 195°C. Anal. Calc. for $C_{35}H_{51}N_2I$: C, 67.08; H, 8.20; N, 4.48. Found: C, 66.60; H, 8.26; N, 4.57. δ H (300 MHz, $CDCl_3$): 0.87 (t, 3H, $1CH_3$), 1.26 (m, 26H, $13CH_2$), 1.56 (m, 2H, $1CH_2$), 3.09 (s, 3H, $1N{-}CH_3$), 3.43 (t, 2H, $1N{-}CH_2$), 4.56 (s, 3H, $1N^+{-}CH_3$), 6.74 (d, 2H, phenyl), 7.58 (d, 1H, 1CH=), 7.63 (d, 2H, phenyl), 7.74 (d, 1H, CH=), 7.88 (d, 1H, quinolyl), 8.04 (m, 2H, quinolyl), 8.11 (m, 2H, quinolyl), 8.62 (d, 1H, quinolyl).

MHQ-6: Yield: 23%. M.p.: 179°C. Anal. Calc. for $C_{35}H_{51}N_2I$: C, 67.08; H, 8.20; N, 4.48. Found: C, 66.46; H, 8.31; N, 4.05. δ H (300 MHz, $CDCl_3$): 0.84 (t, 3H, $1CH_3$), 1.23 (m, 26H, $13CH_2$), 1.60 (m, 2H, $1CH_2$), 3.12 (s, 3H, $1N{-}CH_3$), 3.41 (t, 2H, $1N{-}CH_2$), 4.89 (s, 3H, $1N^+{-}CH_3$), 7.36 (d, 2H, phenyl), 7.57 (d, 1H, 1CH=), 7.62 (d, 2H, phenyl), 7.70 (d, 1H, 1CH=), 7.92 (m, 2H, quinolyl), 8.14 (d, 1H, quinolyl), 8.58 (d, 1H, quinolyl), 8.92 (m, 2H, quinolyl).

Methyl viologen diiodide (MV^{2+}) was synthesized by reaction of 4,4′ − dipyridyl with methyl iodide. Its identity was confirmed by ^{1}HNMR analysis. The electrolyte for the electrochemical experiment was KCl, analytical reagent grade (AR). Hydroquinone (H_2Q) (AR) was recrystallized from water before use. $EuCl_3 \cdot 6H_2O$ was obtained by reaction of Eu_2O_3 with hydrochloric acid. The spreading solvent used for film deposition was chloroform (AR).

C, H, N data of the compounds were obtained by using a Carlo Erba 1106 elemental analyzer. ^1H NMR spectra were measured by using Bruker ARX300. Electronic spectra in solution or in LB films were recorded on a Shimadzu model 3100 UV–vis–NIR spectrophotometer. Melting point was performed on an X4 micromelting point apparatus. SHG experiments were carried out in transmission with the laser beam (Nd:YAG, $\lambda = 1064$ nm) at an angle of 45° to the LB films. The second-harmonic intensities were calibrated against a Y-cut quartz reference ($d_{11} = 0.5$ pmV^{-1}). The data of second-harmonic generation (SHG) from the LB films were analyzed by a general procedure described by Ashwell et al. [20]. Monolayers of MHQ-2, MHQ-4 and MHQ-6 were prepared by spreading the corresponding dye solution on a NIMA 622 Langmuir–Blodgett trough, and the temperature was kept constant at 20 ± 1°C. Details on the method used for pressure (π)–area (A) measurement and transfer process were the same as described previously [21]. Water from an EASY pure RF system was used throughout ($R \sim 18$ MΩ). In all the cases, the transfer ratios were 1.0 ± 0.1.

Photoelectrochemical measurements were carried out in 0.5 M KCl solution using the LB modified ITO electrode, platinum wire and Ag/AgCl electrode as working electrode, counter electrode and reference electrode, respectively. Effective illuminated area of a flat window for MHQ-2, MHQ-4 and MHQ-6 were 0.5, 0.5 and 1 cm^2, respectively. The light source used for the photoelectrochemical study was a 500-W Xe arc lamp; the light beam was passed through a group of filters (ca. 300–800 nm, Toshiba, Japan, and Schott, USA) in order to get a given bandpass of light. The light intensity at each wavelength was measured with an energy and power meter (Scientech, USA). Cyclic voltammetry (CV) experiments were performed on an EG&GPAR 273 potentiostat/galvanostat with EG&GPAR 270 electrochemical software. CV studies for the three dyes were carried out (sweep rate = 100 mV S^{-1}) in 0.5M KCl aqueous solution. Oxygen was removed from the electrolyte solution by bubbling N_2 before every measurement. The quantum chemistry calculation and the structure optimization were done under B3LYP/6–31 G(d) or MPZ/6–31 G(d) level by Gaussian 94.

3. Results and discussion

3.1. LB monolayer film properties

The surface pressure vs. area isotherms of the three dyes (MHQ-2, MHQ-4 and MHQ-6) are given in Fig. 1. The collapse pressures of those molecules are larger than 50 mNm^{-1} and the transfer ratios were 1.0 ± 0.1, indicating that they can form good monolayer films at the air/water interface. The isothermal curve shapes of MHQ-2, MHQ-4 and MHQ-6 show similar trends with increasing pressure, the limiting areas are 0.54, 0.48 and 0.46 nm^2 molecule^{-1}, respectively, extrapolating the solid region to zero surface pressure. The molecule area of MHQ-2 is consistent with the 0.53 nm^2 for the congener *N*-methyl-2-(4-dihexadecylaminostyryl) benzothiazolium iodide[22].

It is well known that the quinolinium group is a hydrophilic group part, so the 2-quinolinium, 4-quinolinium and 6-quinolinium were under the water surface. However, the 2-quinolinium ring has to incline largely due to its rigid structure and the nitrogen in the ring locates closely to the ethenyl bridge. The possible arrangement of three dyes at the air/water interface could be considered as Fig. 2. It shows clearly that the tilt angles are different due to the difference of the positions of the quinolinium

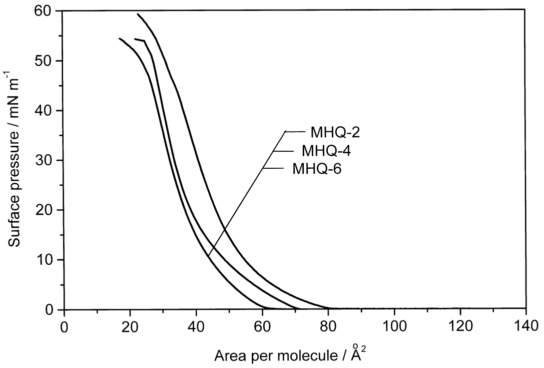

Fig. 1. Surface pressure–area (π–A) isotherms of MHQ-2 (a), MHQ-4 (b) and MHQ-6 (c) at the air/water interface (20 ± 1°C).

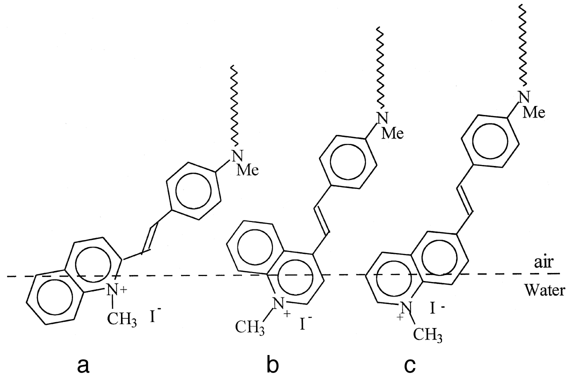

Fig. 2. The possible arrangement of MHQ-2 (a), MHQ-4 (b) and MHQ-6 (c) at the air/water interface.

groups, and it is easy to understand that the sequence of the area per molecule is MHQ-2 > MHQ-4 > MHQ-6.

3.2. Absorption spectra of LB films

The broad absorption maxima of the charge-transfer band of MHQ-2, MHQ-4 and MHQ-6 in chloroform solution peak at 560, 580 and 460 nm, respectively (see Table 1). It can be seen from Scheme 2 that 6-quinolinium group cannot conjugate with 4-*N*-methyl-*N*-hexadecylaminophenylethenyl group while 2-quinolinium and 4-quinolinium groups can conjugate and extend their conjugation systems. The quantum chemistry calculation for a model molecule (Scheme 3) which is the electron-accepting group, shows that the charge density of 6-positional carbon in quinolinium ring is much smaller than that of 2-positional carbon and 4-positional carbon, which confirms the above conclusion. Extension of the conjugation system, in general, results in red shift of the absorption maximum of electric spectra, λ_{max} [23]. This is the reason why the absorption maximum of MHQ-6 in $CHCl_3$ solution $\lambda_{max(s)}$is blue-shifted in comparison with those of MHQ-2 and MHQ-4. Compared their electronic spectra of LB film on the ITO (see Fig. 3) with those in the chloroform solution, λ_{max} blue shift of 45 nm, 50 nm and 85 nm can be observed for MHQ-2, MHQ-4 and MHQ-6, respectively, which results from the extended dipole interactions between the chromophores. The blue shifts suggest formation of H-aggregates on the ITO LB films for MHQ-2, MHQ-4 and MHQ-6 [24]. Similar aggregation behavior for the three dyes deposited on quartz has also been observed.

3.3. Second harmonic generation (SHG) properties

The second harmonic intensities for MHQ-2, MHQ-4 and MHQ-6 LB films deposited on quartz under 35 mNm^{-1} are 197 pmV^{-1}, 292 pmV^{-1} and 40 pmV^{-1}, respectively. In order to discuss further the difference of their SHG properties, we use the theory of Levine [25] and Oudar et al. [26] to deal

Table 1
Data of MHQ-2, MHQ-4 and MHQ-6 LB Film Properties
I: Photocurrent per area; η: external quantum yield; φ: tilt angle of the molecule in LB film; $\chi^{(2)}$: second harmonic intensity; *A*: area per molecule; λ_{max}: maximum wavelength (s and f stand for in solution and in LB film, respectively).

Dye	I^a ($nA\ cm^{-2}$)	I^b ($nA\ cm^{-2}$)	η^b (%)	I^c ($nA\ cm^{-2}$)	η^c (%)	I^d ($nA\ cm^{-2}$)	η^d (%)	I^e ($nA\ cm^{-2}$)	η^e (%)	$\chi^{(2)}$ (pmV^{-1})	φ (degree)	A (nm^2)	$\lambda_{max(s)}$ (nm)	$\lambda_{max(f)}$ (nm)
MHQ-2	1050–1314	43	0.57	57	0.75	86.5	1.15	178.4	2.36	197	45	0.54	561	516
MHQ-4	2408–2860	84	0.68	134.4	1.09	204.6	1.66	371.8	3.06	292	37	0.48	580	560
MHQ-6	282–375	10	0.12	12.5	0.15	17.6	0.21	33.2	0.40	40	36	0.46	480	375

[a] Irradiated under 137 mW cm^{-2} white light, in 0.5 M KCl electrolyte solution containing dissolved O_2.

[b] Irradiated under 137 mW cm^{-2} white light at 500, 550 and 350 nm for MHQ-2, MHQ-4 and MHQ-6, respectively, in 0.5 M KCl electrolyte solution containing dissolved O_2.

[c] Irradiated under 137 mW cm^{-2} white light at 500, 550 and 350 nm for MHQ-2, MHQ-4 and MHQ-6, respectively, in 0.5 M KCl electrolyte solution containing dissolved O_2 and 1 mM MV^{2+}.

[d] Irradiated under 137 mW cm^{-2} white light at 500, 550 and 350 nm for MHQ-2, MHQ-4 and MHQ-6, respectively, under −100mV, dissolved O_2 and 1 mM MV^{2+}.

[e] Irradiated under 137 mW cm^{-2} white light at 500, 550 and 350 nm for MHQ-2, MHQ-4 and MHQ-6, respectively, under −100mV, pH = 2, dissolved O_2 and 8 mM MV^{2+}.

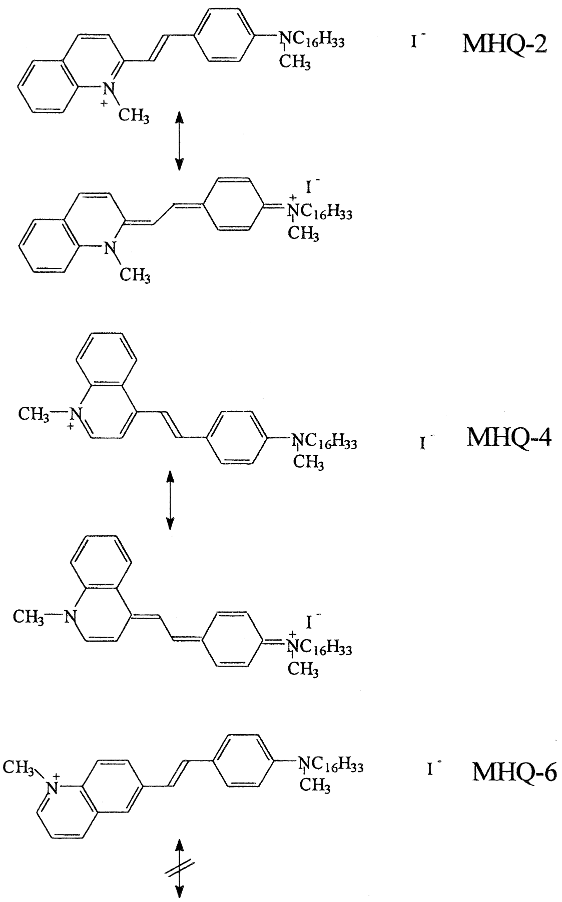

Scheme 2. Diagram showing the three resonant structures.

with these dyes MHQ-2, MHQ-4 and MHQ-6. The contributions to β can be separated into two parts for the dyes.

$$\beta = \beta_{\mathrm{add}} + \beta_{\mathrm{CT}}$$

where β_{add} is an additive part due to substitute-induced asymmetry in the charge distribution and β_{CT} is the charge-transfer term. It is well known from Scheme 2 that β_{CT} of MHQ-6 is almost zero and therefore is much smaller than β_{CT} of MHQ-2 and MHQ-4, which explain why $\chi^{(2)}$ of MHQ-6 is smallest in three dyes. In our experiment the wavelength of resonant enhancement is 532 nm, and $\Delta\lambda_{\mathrm{max}}$ ($\Delta\lambda_{\mathrm{max}}$ stands for $\lambda_{\mathrm{max(f)}} - 532$ nm) for MHQ-2, MHQ-4 and MHQ-6 are -16, 28 and -157 nm, which shows the sequence of resonant enhancement is MHQ-2 > MHQ-4 > MHQ-6, since the larger the shift towards red or blue is, the smaller the resonant enhancement of the dyes is. Therefore, the larger $\chi^{(2)}$ of MHQ-4 is not mainly due to its resonant enhancement but its structural factor. This result shows that the 4-quinolinium is a good electron-accepting group.

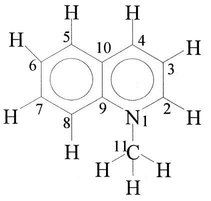

Scheme 3. The model molecule for quantum chemistry calculation.

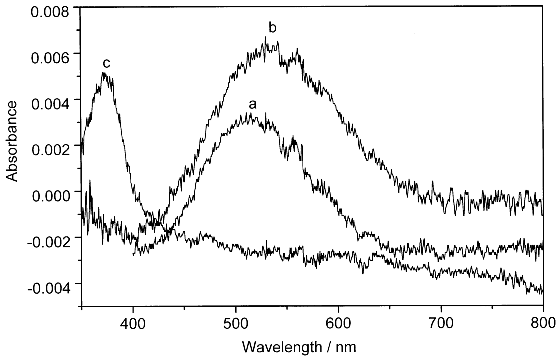

Fig. 3. UV–vis absorption spectra of the dyes in LB monolayers on ITO electrode. (a) MHQ-2; (b) MHQ-4; (c) MHQ-6.

3.4. Photoelectric conversion (PEC) properties

A steady cathodic photocurrent was obtained from the dye monolayer-modified ITO electrode in 0.5M KCl solution by illumination of 137 mW cm^{-2} white light. The agreement between the action spectra (see Fig. 4) and absorption spectra of the three dyes (see Fig. 3) in 300–700 nm implies that the aggregates of the dyes in the LB films are responsible for photocurrent generation. In order to understand the flow of electrons between ITO electrode and electrolyte solution, the effect of experimental conditions, such as applied electrode potential, concentration of the electron acceptor or donor, pH of the electrolyte, was investigated under the same conditions.

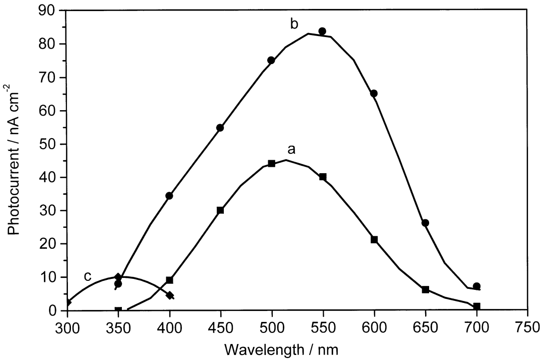

Fig. 4. Action spectra for the cathodic photocurrents. The intensities at different wavelengths are all normalized. (a) MHQ-2; (b) MHQ-4; (c) MHQ-6.

3.5. Dependence of PEC on experimental conditions

The photocurrent vs. bias voltage curves for MHQ-2, MHQ-4 and MHQ-6 LB modified ITO electrodes are shown in Fig. 5. Comparing the curves (a), (b) and (c) with curve (d), the dark current is meager, indicating that the current is generated by the light-sensitized dye molecules. Due to an enhancement of the rate constant for charge transfer or an efficient dissociation of electron–hole pairs, the cathodic photocurrent is increased with the increasing of the applied bias potential when the negative bias voltage is applied to ITO electrode, indicating that the photocurrent flows in the same direction as the applied negative voltage.

The dependence of photocurrent on the nature of the redox component in the electrolyte solution can help us to understand the mechanism of PEC. Our experiment results indicate that the electron acceptors (MV^{2+} and O_2) in the systems sensitize the photocurrent and the electron donors (H_2Q and N_2) quench the photocurrent for three dyes. For example, Fig. 6 shows a plot of the photocurrent for MHQ-2 vs. the concentration of $EuCl_3$ which acts as electron acceptor, illustrated by the 102 mW cm^{-2} white light and without any bias voltage, in 0.5M KCl electrolyte solution. The cathodic photocurrent increased gradually with increasing concentration of $EuCl_3$. The leveling of the increasing effect began at 0.8 mmol dm^{-3}, and a photocurrent of 880 nA cm^{-2} was obtained with irradiation of 30.5 mW cm^{-2} white lightl; the external quantum yield is 1.34%. This means that $EuCl_3$ acted as a supersensitizer in accepting electrons from the MHQ-2 assemblies and therefore increased the concentration of electrons involved in the electron-transfer process. Similar results were obtained for the MHQ-4 and MHQ-6 modified ITO electrodes.

In order to understand the effect of the acid or base character of medium on the photocurrent generation, the effect of pH value was investigated in a Britton–Kobinson buffer solution containing 0.5 M KCl (see Fig. 7). The results show that the change tendencies of the photocurrent under zero bias voltage for MHQ-2, MHQ-4 and MHQ-6 are similar and their photocurrent decreases rapidly with increasing

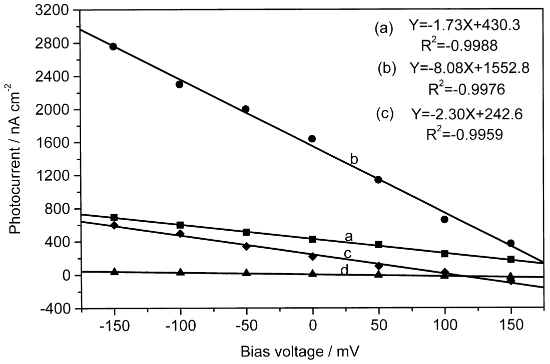

Fig. 5. Diagram of photocurrent vs. bias voltage for MHQ-2 (a), MHQ-4 (b) and MHQ-6 (c) LB films-ITO electrodes in 0.5 M KCl aqueous solution under ambient conditions, upon irradiation with white light at 102 mW cm^{-2}; (d) Dark current.

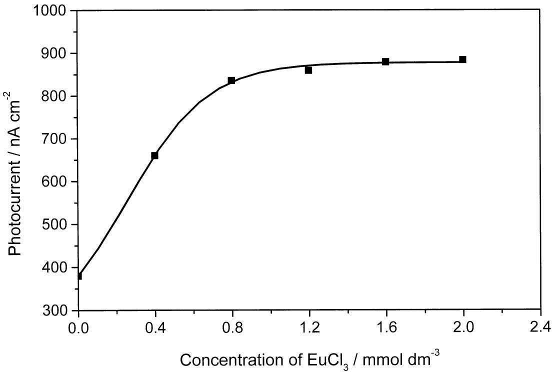

Fig. 6. Dependence of the photocurrent on the concentration of $EuCl_3$ under ambient conditions for MHQ-2 monolayer upon irradiation with white light at 30.5 mW cm^{-2}.

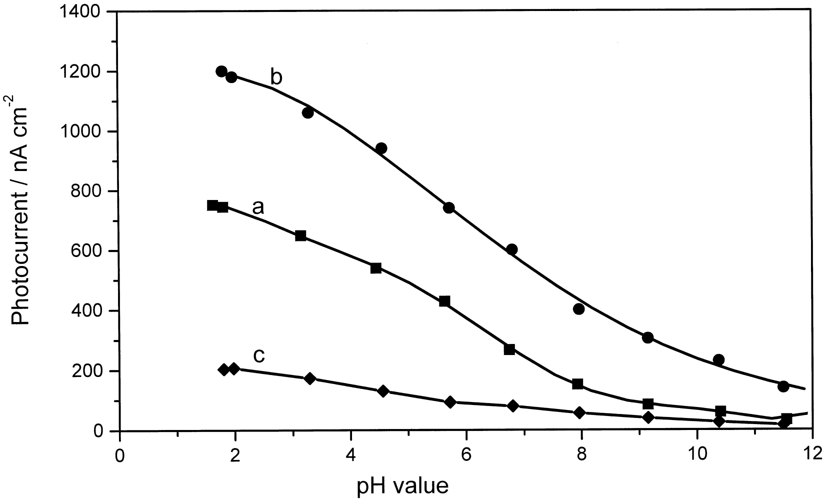

Fig. 7. Effect of pH on photocurrent for MHQ-2 (a), MHQ-4 (b) and MHQ-6 (c) electrode in Britton–Kobison buffer solution containing 0.5 M KCl without bias voltage under ambient conditions, upon irradiation with white light at 30.5 mW cm^{-2}.

pH value. This is attributed to the fact that an acidic medium can lead an anodic shift of the flat-band potential of the ITO electrode. On the contrary, the alkaline medium can produce the cathodic shift of the flat-band potential of the ITO electrode. Under favorable conditions, e.g. pH = ca. 2, in the presence of O_2 and 8 mM MV^{2+}, with −100 mV bias voltage, then a photocurrent of 178.4 nA cm^{-2} for the MHQ-2 was obtained under irradiation at 500 nm wavelength; the external quantum yield of MHQ-2 was 2.36%, while in the same electrolyte conditions, the external quantum yields were 3.06% and 0.40% for MHQ-4 and MHQ-6 under irradiation at 550 and 350 nm, respectively (Table 1, I^e, ηe).

3.6. Mechanism of PEC

In order to understand the photocurrent generation mechanism, the energy levels of the relevant electronic states must be estimated. The oxidation potential data for the dye LB films obtained from the CV provide the energy level of the HOMO, and the UV–vis spectra of the dye LB films provide the energy gap of the excited state and ground state. Therefore, the energy level of the ground state can be known. The CV study indicated that the oxidation peak potentials are 0.94, 0.88 and 0.75V for MHQ-2, MHQ-4 and MHQ-6, respectively. The energy levels of the ground state and excited state of the MHQ-2 film (as an example) are assumed to be −5.68 eV (0.94 V vs. SCE) and −3.28 eV on the absolute scale, respectively, with reference to its oxidation potential of 0.94 V (vs. SCE) and band gap of 2.40 eV (516 nm). The conduction band (E_c) and valence band (E_v) edges of ITO electrode surface are estimated to be ca. −4.5 and −8.3 eV [27], respectively. Reduction potential of MV^{2+} is −4.51 eV (−0.23 V vs. SCE) [28] and oxidation potential of H_2Q is −4.61 eV (−0.13 V vs. SCE) [28] on the absolute scale. An energy level diagram which describes the mechanism for photosensitization of the dye ITO electrode can be constructed as shown in Scheme 4.

It is well known that the direction of the photocurrent depends not only on the dye sensitized by light but also on nature of the redox couple in the aqueous phase surrounding the electrode. In the presence of some electron acceptors, such as O_2, MV^{2+}, Eu^{3+} and acidic medium in electrolyte solution, electrons transfer from the excited state of MHQ-2 to the electron acceptor, subsequently the electrons of ITO conduction band inject into the hole residing in the dye aggregate. Thus, cathodic photocurrent is generated. On the contrary, if there are strong electron donors in the system, such as H_2Q, it will exhibit a reduced cathodic photocurrent and even redirect to

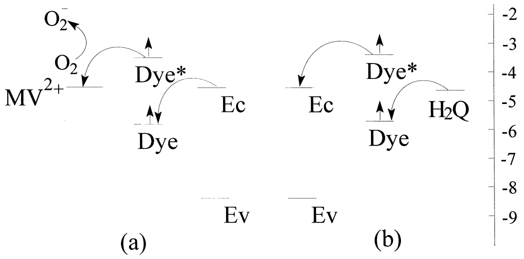

Scheme 4. Mechanism of electron transfer of the dye on ITO electrode in different conditions. (a) cathodic photocurrent; (b) anodic photocurrent. MHQ-2 and MHQ-2* present the ground state and the excited state of the dye MHQ-2, respectively.

an anodic photocurrent. The same mechanism for MHQ-4 and MHQ-6 is proposed.

4. Conclusion

(1) From Table 1, one can conclude that the sequence of second-harmonic intensity $\chi^{(2)}$ is MHQ-4 > MHQ-2 > MHQ-6, and the external quantum yield of the photocurrent has similar sequence for the three dye molecules. It can be concluded that the higher the molecular NLO hyperpolarizability is, the better the molecular PEC efficiency in the hemicyanine analogues will be. Further work on the relationship between SHG and PEC properties is in preparation.

(2) The intramolecular photoinduced electron transfer (PET) through CH=CH bond is the key to SHG and PEC properties. The different π-conjugation degrees of the organic molecules affects the generation of PET. The dependence of SHG property on the different conjugation degree of *o*-, *m*- and *p*-substitution of various nitroanilines has been reported [17]. Here, there is a great difference of π-conjugation degrees in MHQ-2, MHQ-4 and MHQ-6 systems and their SHG and PEC properties differ greatly, indicating that the different π-conjugation degrees result in large differences in SHG and PEC properties. To our knowledge, the effect of π-conjugation degree on PEC property was firstly investigated.

(3) These experimental results show that 4-quinolinium as electron acceptor is more effective than 2-quinolinium and 6-quinolinium, indicating that the relative position of the same substitutent affects SHG and PEC properties.

Acknowledgements

The authors thank the State Key Project of Fundamental Research (G1998061300) and National Natural Science Foundation of China (29671001, 29671003) for financial support of this work.

References

[1] M. Fujihira, in: New Functionality Materials, Elsevier, Amsterdam, 1993.

[2] W.E. Moerner, S.M. Silence, Chem. Rev 94 (1994) 127.

[3] R. Clément, P.G. Lacrox, D. O'Hare, J. Evans, Adv. Mater. 6 (1994) 794.

[4] P.G. Lacrox, R. Clément, K. Nakatani, J. Zyss, I. Ledoux, Science 263 (1994) 658.

[5] S. Bernard, P. Yu, T. Coradin, E. Rivière, K. Nakatani, R. Clément, Adv. Mater. 9 (1997) 981.

[6] P.G. Lacrox, K. Nakatani, Adv. Mater. 9 (1997) 1105.

[7] R. Andreu, I. Malfant, P.G. Lacroix, H. Gornitzka, Chem. Mater. 11 (1999) 840.

[8] W.S. Xia, C.H. Huang, D.J. Zhou, Langmuir 13 (1997) 80.

[9] W.S. Xia, .H. Huang, X.Z. Ye, C.P. Luo, L.B Gan, Z.F. Liu, J. Phys. Chem. 100 (1996) 2244.

[10] A.D. Lang, J. Zhai, C.H. Huang, L.B. Gan, Y.L. Zhao, D.J. Zhou, Z.D. Chen, J. Phys. Chem. B 102 (1998) 1424.

[11] D.G. Wu, C.H. Huang, L.B. Gan, W. Zhang, J. Zheng, J. Phys. Chem. B 103 (1999) 4377.

[12] D.G. Wu, C.H. Huang, Y.Y. Huang, L.B. Gan, A.C. Yu, X.S. Zhao, J. Phys. Chem. B 103 (1999) 7130.

[13] J.L. Brédas, Science 263 (1994) 487.

[14] S.R. Marder, L.-T. Cheng, B.G. Tiemann, C.F. Andrienne, M. Blanchard-Desce, J.W. Perry, J. Skindhoj, Science 263 (1994) 511.

[15] D.M. Burland, J. Downing, J. Michl, Mol. Cryst. Liq. Cryst. Sci. Technol., Sect. B. Nonlinear Optics 3 (1992) 195.

[16] D.R. Kanis, M.A. Ratner, T.J. Marks, Chem. Rev. 94 (1994) 195.

[17] D.J. Williams, Angew. Chem., Int. Ed. Engl. 23 (1984) 690.

[18] A. Hassner, D. Birnbaum, L.M. Loew, J. Org. Chem 49 (1984) 2546.

[19] H. Wang, L. Xu, B. Zhang, Y. Cao, Chem. Res. Kaifeng, People's Repub. China 8 (1997) 1.

[20] G.J. Ashwell, P.D. Jackson, D. Lochum, W.A. Crossland, P.A. Thrompson, G.S. Bahra, C.R. Brown, C. Jasper, Proc. R. Soc. London, Ser. A 445 (1994) 385.

[21] D.G. Wu, C.H. Huang, L.B. Gan, Y.Y. Huang, Langmuir 14 (1998) 3783.

[22] J. Zheng, D.G. Wu, J. Zhai, C.H. Huang, W.W. Pei, X.C. Gao, Phys. Chem. Chem. Phys. 1 (1999) 2345.

[23] M.J.S. Dewar, J. Chem. Soc. (1950) 2329.
[24] W.F. Mooney, P.E. Brown, J.C. Russell, S.B. Costa, L.G. Pedersen, D.G. Whitten, J. Am. Chem. Soc. 106 (1984) 5659.
[25] B.F. Levine, Chem. Phys. Lett. 37 (1976) 516.
[26] J.L. Oudar, D.S. Chemia, J. Chem. Phys. 66 (1977) 2664.
[27] L. Sereno, J.J. Silber, L. Otero, M.D.V. Bohorquez, A.L. Moore, T.A. Moore, D. Gust, J. Phys. Chem. 100 (1996) 814.
[28] Y.S. Kim, K. Liang, K.Y. Law, D.G. Whitten, J. Phys. Chem. 84 (1994) 984.